CHAPTER IV

RESULTS AND DISCUSSION

4.1 Synthesis of chelating ligands

Two chelating ligands, AEPE and AEEE, were synthesized. These ligands were different in number of carbon atom between two adjacent sulfur atoms.

4.1.1 2-[3-(2-Amino-ethylsulfanyl)-propylsulfanyl]-ethylamine (AEPE)

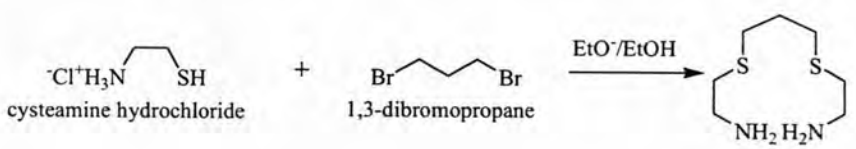

Scheme 4.1 Synthesis of AEPE.

AEPE was synthesized from the reaction between cysteamine hydrochloride and 1,3-dibromopropane via nucleophilic substitution reaction. Synthesis of AEPE was shown in Scheme 4.1. Nucleophile was generated by ethoxide that abstracted proton of –SH and then reacted with 1,3-dibromopropane which has bromide as leaving groups. The synthesis of AEPE was done at the mole ratio of cysteamine hydrochloride : 1,3-dibromopropane equal to 2:1. The product was obtained as yellow oil. The yield of AEPE was 79 %.

The ^{1}H-NMR spectrum of AEPE was recorded in $CDCl_3$. ^{1}H-NMR spectrum of aliphatic proton region showed 3 multiplets due to symmetrical structure of chelating ligand as follows: δ (ppm) 1.77 (2H, *t*, $CH_2C\underline{H}_2CH_2$, J = 7.02 Hz), 2.53 (8H, *t*, $SC\underline{H}_2$, J = 6.24 Hz) and 2.78 (4H, *t*, $C\underline{H}_2NH_2$, J = 6.24 Hz). The ^{1}H-NMR spectrum of AEPE is presented in Figure A.1.

The ^{13}C-NMR spectrum of AEPE was obtained with chemical shifts as followed: δ (ppm) 29.40 (1C, s, $CH_2\underline{C}H_2CH_2$), 30.46 (2C, s, $S\underline{C}H_2CH_2NH_2$), 36.18 (2C, s, $CH_2CH_2\underline{C}H_2S$) and 41.02 (2C, s, $NH_2\underline{C}H_2CH_2$). The ^{13}C-NMR spectrum of AEPE is presented in Figure A.2.

The FT-IR spectrum of AEPE showed absorption bands of primary amine N-H stretching at 3354-3280 cm^{-1}, primary amine N-H bending at 1592 cm^{-1}, primary amine C-N stretching at 1069 cm^{-1}, aliphatic C-H stretching at 2856-2915 cm^{-1}, aliphatic C-H bending at 1344 cm^{-1}. The FTIR spectrum of AEPE is illustrated in Figure A.3.

The results indicated that AEPE was successfully synthesized.

4.1.2 2-[2-(2-Amino-ethylsulfanyl)-ethylsulfanyl]-ethylamine (AEEE)

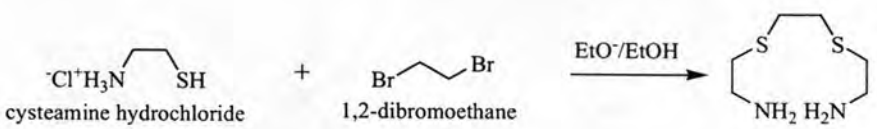

Scheme 4.2 Synthesis of AEEE.

Preparation of AEEE was done by the same methodology of AEPE but 1,3-dibromopropane was replaced with 1,2-dibromoethane with the same mole ratio of cysteamine hydrochloride : 1,2-dibromoethane equal to 2:1. The product was obtained as yellow oil. The yield of AEEE was 60 %. The synthesis of AEEE was shown in Scheme 4.2.

The ^{1}H-NMR spectrum of AEEE was recorded in $CDCl_3$. Aliphatic proton region showed 3 multiplets due to symmetrical structure of chelating ligand as follows: δ (ppm) 2.83 (4H, *t*, $NH_2C\underline{H}_2CH_2$, J = 6.24 Hz), 2.67 (4H, *s*, $SC\underline{H}_2CH_2S$) and 2.60 (4H, *t*, $SC\underline{H}_2CH_2NH_2$, J = 6.24 Hz). The ^{1}H-NMR spectrum of AEEE is presented in Figure A.4.

The ^{13}C-NMR spectrum of AEEE was obtained with chemical shifts as followed: δ (ppm) 41.18 (2C, s, $NH_2\underline{C}H_2CH_2$), 36.36 (2C, s, $SCH_2\underline{C}H_2S$) and 31.92 (2C, s, $S\underline{C}H_2CH_2NH_2$). The ^{13}C-NMR spectrum of AEPE is presented in Figure A.5.

The FT-IR spectrum of AEEE was almost similar to AEPE. It showed absorption bands of primary amine N-H stretching at 3349-3285 cm^{-1}, primary amine N-H bending at 1591 cm^{-1}, primary amine C-N stretching at 1072 cm^{-1}, aliphatic C-H stretching at 2907-2817 cm^{-1}, aliphatic C-H bending at 1452 cm^{-1}. The FT-IR spectrum of AEEE is illustrated in Figure A.6.

The results indicated that AEEE was successfully synthesized.

4.2 Preparation and characterization of chelating polystyrene-divinylbenzene

4.2.1 Preparation of aldehydic polystyrene-divinylbenzene

In the first step in preparation of chelating resins. Polystyrene-divinylbenzene with aldehyde functional groups (CHO-PS-DVB) has been prepared by oxidizing 1 % cross-linked chloromethylated polystyrene-divinylbenzene (Cl-PS-DVB, white colored beads) with dimethylsulfoxide and sodium hydrogen carbonate at 155 °C for 6 hours as shown in Scheme 4.3. CHO-PS-DVB was obtained in pale-yellow beads.

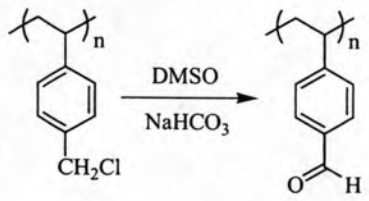

Scheme 4.3 Oxidation of chloromethylated polystyrene-divinylbenzene.

A yield of dimethylsulfoxide oxidation can be estimated by measuring the nitrogen content of its oxime derivative (Oxime-PS-DVB). CHO-PS-DVB was transformed into oxime by reaction with excess hydroxylamine hydrochloride (0.3 g) in 5 ml of pyridine for 6 hours at 90-100 °C as shown in Scheme 4.4. The result of nitrogen content by elemental analysis was discussed in 4.2.2.4.

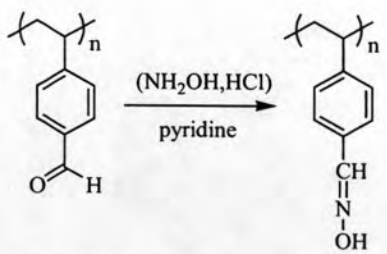

Scheme 4.4 Conversion of aldehydric polystyrene-divinylbenzene into its oxime derivative.

4.2.2 Characterization of aldehydic polystyrene-divinylbenzene

All resins obtained in 4.2.1 were characterized by FT-IR, FT-Raman spectroscopy, thermogravimetric analysis and elemental analysis.

4.2.2.1 FT-IR spectroscopy

FT-IR spectrum of Cl-PS-DVB was shown in Figure 4.1 (a). Absorption bands of C-H aliphatic stretching appeared between 2920-2853 cm^{-1} and aromatic C-H stretching peaks between 3053-3022 cm^{-1}. The C-Cl stretching vibration appeared around 669,705 cm^{-1}. The C=C stretching of aromatic absorption band appeared around 1606-1449 cm^{-1}.

In Figure 4.1 (b), a spectrum of CHO-PS-DVB showed two important peaks which were significantly different from the spectrum of Cl-PS-DVB. These were an intense C=O absorption band at 1695 cm^{-1} and aldehydric C-H stretching absorption at 2718 cm^{-1}. However, there were remain some chloride group from the appearance of the weak intensity of C-Cl stretching vibration peak.

Conversion of CHO-PS-DVB into its oxime seemed to be quantitative because in FTIR spectrum of Oxime-PS-DVB in Figure 4.1 show no C=O stretching absorption peak.

4.2.2.2 FT-Raman spectroscopy

FT-Raman spectroscopy was used to confirm structure of resins. Raman spectra of Cl-PS-DVB and CHO-PS-DVB were shown in Figure 4.2 (a) and (b), respectively. Raman spectrum of both resins showed similar results as FT-IR spectra. In Figure 4.2 (a), the spectrum of Cl-PS-DVB was shown the important peaks such as C-H aliphatic str at 2850-2955 cm^{-1}, C-H str of aromatic at 3002-3051 cm^{-1}, C=C str of aromatic at 1609 cm^{-1}, υ(CC) of aromatic at 999 cm^{-1} and υ(C-Cl) str at 636,673 cm^{-1}. In Figure 4.2 (b), the important peaks was almost similar with 4.2 (a) but there was an important peak C=O vibration at 1698 cm^{-1}, aldehydric C-H stretching scattering was observed as weak scattering at 2715 cm^{-1} and remained υ(C-Cl) as weak intensity.

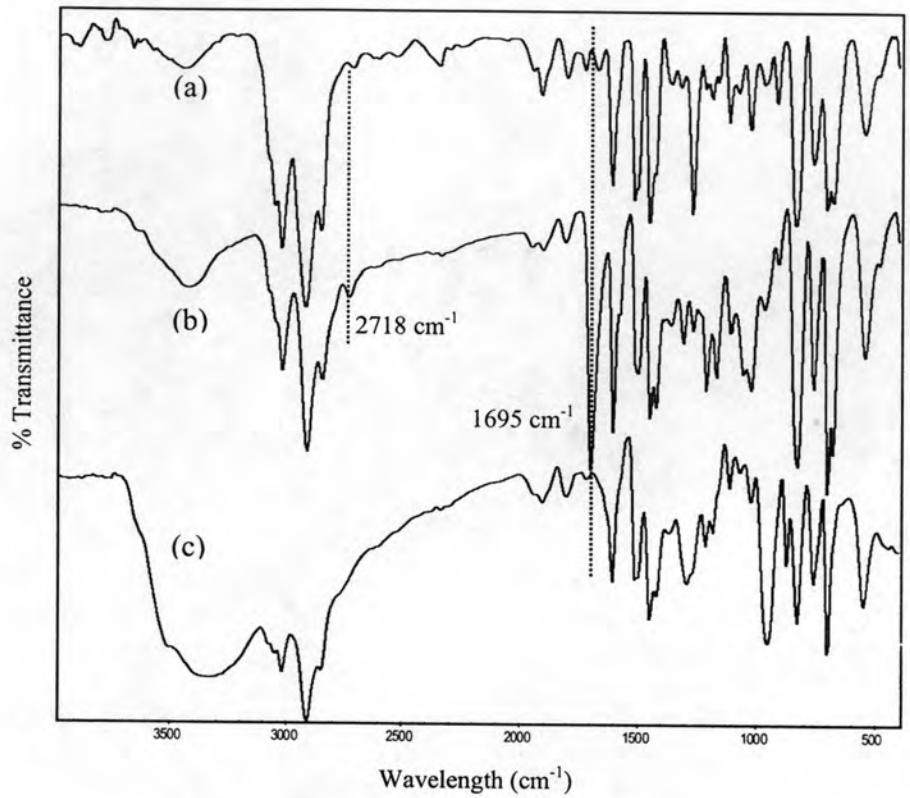

Figure 4.1 FT-IR spectra of (a) chloromethylated polystyrene-divinylbenzene (b) aldehydric polystyrene-divinylbenzene and (c) oxime polystyrene-divinylbenzene.

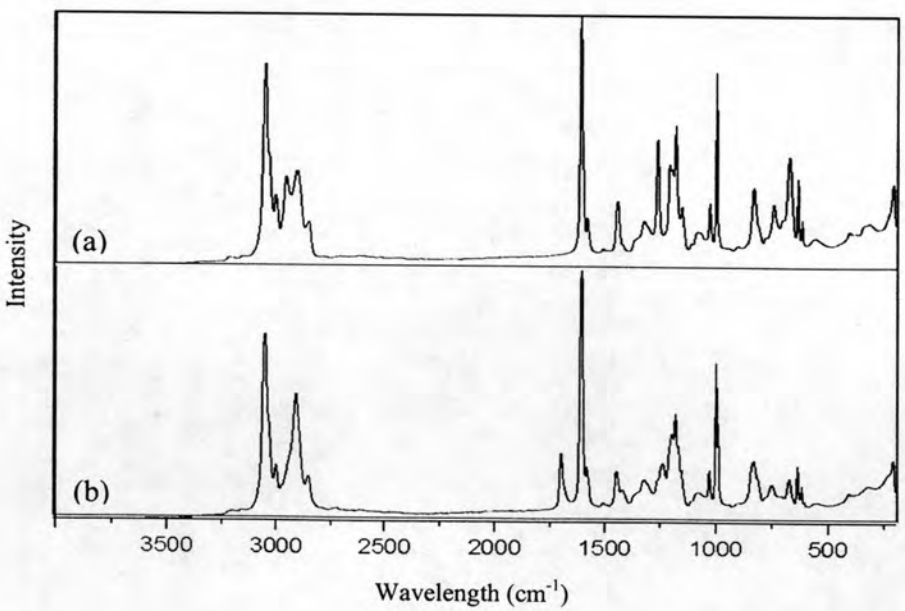

Figure 4.2 Raman spectra of (a) chloromethylated polystyrene-divinylbenzene and (b) aldehydric polystyrene-divinylbenzene.

4.2.2.3 Thermogravimetric analysis

Thermal stability of the resins was investigated using thermogravimetric analysis (TGA). TGA curves of Cl-PS-DVB and CHO-PS-DVB were displayed in Figure 4.3. TGA curves of two resins show many steps of degradation. The initial decomposition temperature (IDT) of resins was found to be in the range of 178-240 °C. The temperature at 50% weight loss of Cl-PS-DVB occurred at higher temperature than CHO-PS-DVB. The maximum rate of weight loss occurred around 400-500 °C might be a degradation of polymeric support. The degradation temperature of Cl-PS-DVB was higher than the modified resin. TGA thermograms indicated that Cl-PS-DVB was more thermal stable than CHO-PS-DVB.

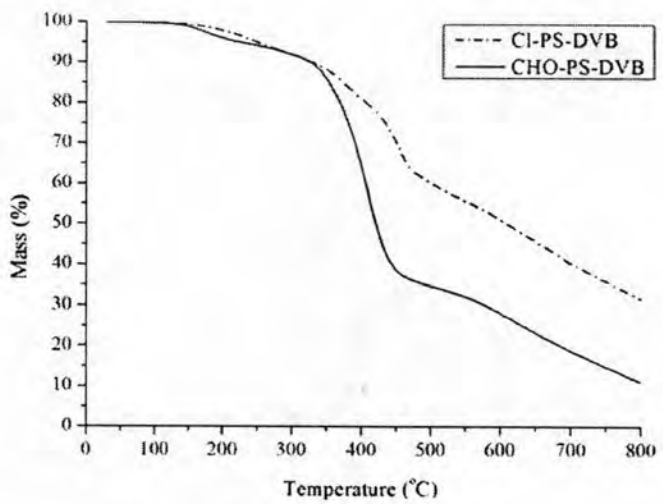

Figure 4.3 TGA thermograms of Cl-PS-DVB and CHO-PS-DVB.

4.2.2.4 Elemental analysis

The elemental analysis results of Cl-PS-DVB and CHO-PS-DVB were not significantly different. From elemental analysis result of Oxime-PS-DVB, it was shown that this resin contained 3.52 % of nitrogen content which corresponds to 2.51 mmol of aldehyde group/g of resin. This was indicated a yield of 57 % for oxidation of Cl-PS-DVB.

The elemental analysis results were shown in Table 4.1.

Table 4.1 Elemental analysis results of Cl-PS-DVB, CHO-PS-DVB and Oxime-PS-DVB

Sample	C (%)	H (%)	N (%)
Cl-PS-DVB	76.39	6.98	-
CHO-PS-DVB	80.91	7.85	-
Oxime-PS-DVB	78.62	7.68	3.52

4.3 Preparation of chelating polymers

Three chelating polymers have been prepared from condensation reaction between primary amine in chelating ligands and aldehyde functionality in polymer converting to Schiff base (imine) linkage. Three chelating ligands used in the preparation of chelating polymers were AEPE, AEEE and triethylenetetramine (TETA).

The conditions of reaction such as reaction times, amount of chelating ligands and the temperature of reaction were studied. The amount of chelating ligands was calculated by assuming that the yield of oxidation of chloromethylated polystyrene-divinylbenzene was 100 %, so the aldehyde group was obtained at 4.42 mmol/g resin. Two molar of aldehyde group was required for coupling with one molar of chelating ligand. Thus, the amounts of chelating ligands were 2.21 mmol/g of resin multiplied with 1.2, 1.5, 1.75, and 2 times (2.65, 3.32, 3.87, and 4.42 mmol/g resin).

The progress of reaction was investigated by FT-IR spectroscopy. The reaction progress could be observed by the disappearance of the C=O absorption band at 1695 cm^{-1} and the appearance of a new C=N absorption band at 1645 cm^{-1}.

4.3.1 Polystyrene containing Schiff base AEPE ligand, AEPE-PS-DVB

AEPE-PS-DVB was synthesized from the reaction between AEPE and CHO-PS-DVB as shown in Scheme 4.5.

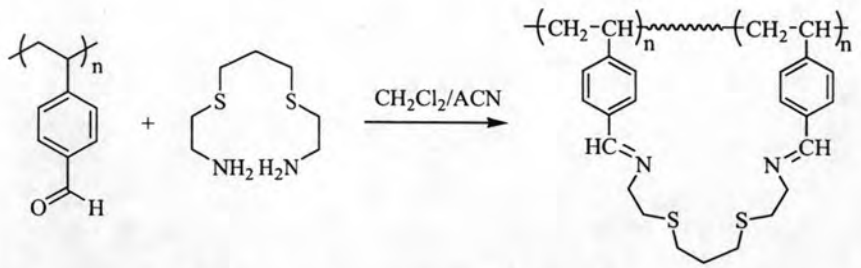

Scheme 4.5 Preparation of AEPE-PS-DVB.

The reaction time was varied between 0-6 hours and done at room temperature with mole of AEPE at 2.65 mmol/g resin. The intensity of the C=O absorption band slightly decreased with increasing of reaction time from 2 to 6 hours as shown in Figure 4.4. The appropriate reaction time was chosen at 6 hours in order to obtain more complete reaction.

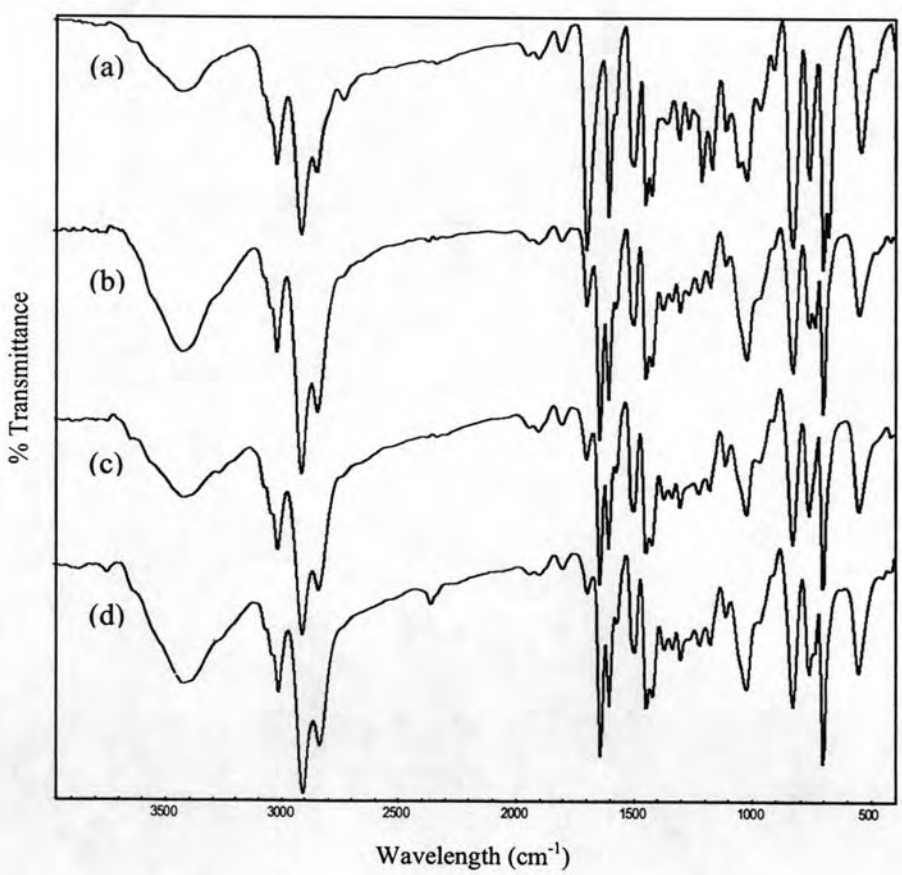

Figure 4.4 FT-IR spectra of the reaction mixture of CHO-PS-DVB with AEPE at different reaction times (a) 0 h (b) 2 hrs (c) 4 hrs, and (d) 6 hrs.

Subsequently, at appropriate reaction time, the reaction was performed at room temperature with different amount of AEPE as shown in Figure 4.5. This was done to investigate the appropriate amount of chelating ligand by monitoring the degree of disappearance of the C=O absorption band. However, the experimental results in Figure 4.5 indicated that increasing in the amount of chelating ligand did not decrease C=O absorption band significantly. Thus, 1.2 times (2.65 mmol/g resin) was an enough amount of AEPE.

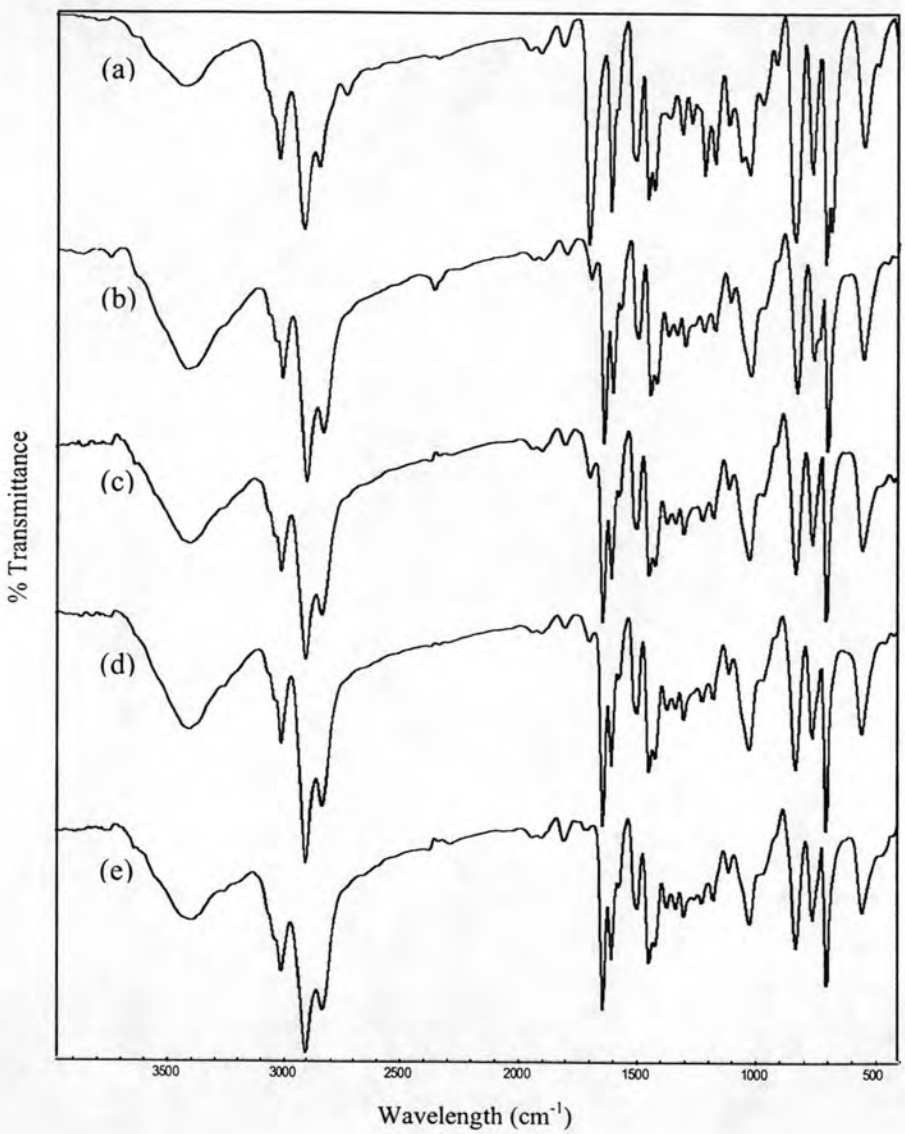

Figure 4.5 FT-IR spectra of the reaction mixture of CHO-PS-DVB with AEPE at different amount of AEPE (a) 0 (b) 2.64 (c) 3.32 (d) 3.87, and (e) 4.42 mmol/g resin.

In order to study the effect of reaction temperature towards the completeness of the reaction, the mixture was done at the same way as the above method except it was refluxed at 50 °C. The experimental results were shown in Figure 4.6. When compared with the above results in Figure 4.5, the intensity of C=O absorption band of each amount of AEPE slightly decreased. In addition, there was no significant decreasing in intensity of C=O absorption band when increased the amount of ligand. However, the reaction was preferably refluxed for more completion.

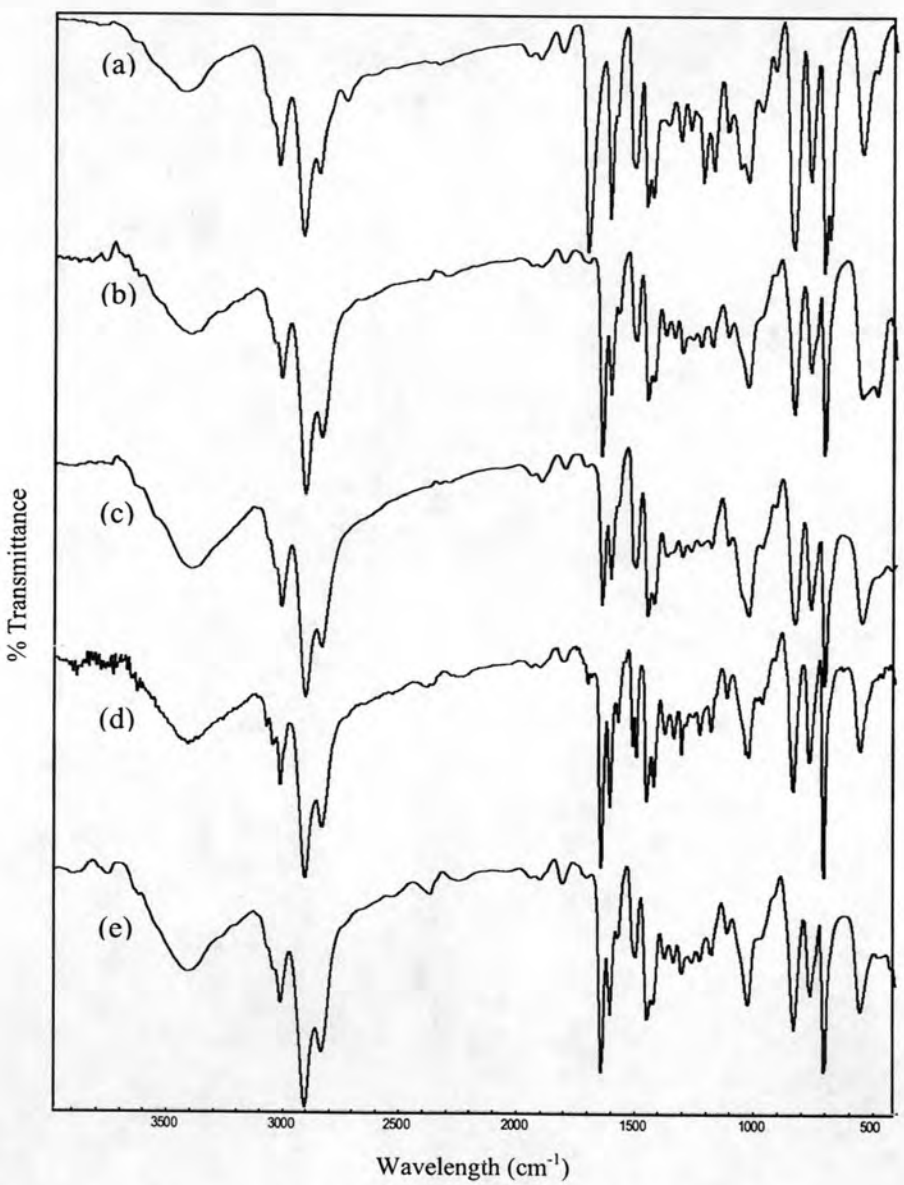

Figure 4.6 FT-IR spectra of the reaction mixture of CHO-PS-DVB with AEPE at 50 °C (a) 0 (b) 2.65 (c) 3.32 (d) 3.87, and (e) 4.42 mmol/g resin.

4.3.2 Polystyrene containing Schiff base AEEE ligand, AEEE-PS-DVB

AEEE-PS-DVB was synthesized from the reaction between AEEE and CHO-PS-DVB as shown in Scheme 4.6.

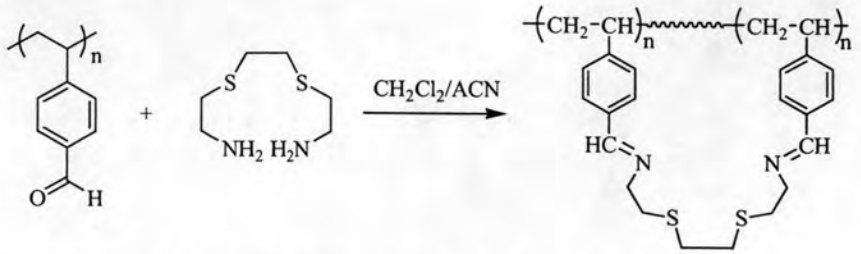

Scheme 4.6 Preparation of AEEE-PS-DVB.

The condition of reaction used in preparation of AEPE-PS-DVB was applied in this preparation, except the study of effect of reaction time. The appropriate reaction time was chosen from the preparation of AEPE-PS-DVB. FT-IR spectra of the product from reaction of CHO-PS-DVB with AEEE at room temperature and the amount of AEEE at 2.65 mmol/g were shown in Figure 4.7. However, at chosen time in Figure 4.7 (b), C=O absorption weak intensity band remained in the spectrum.

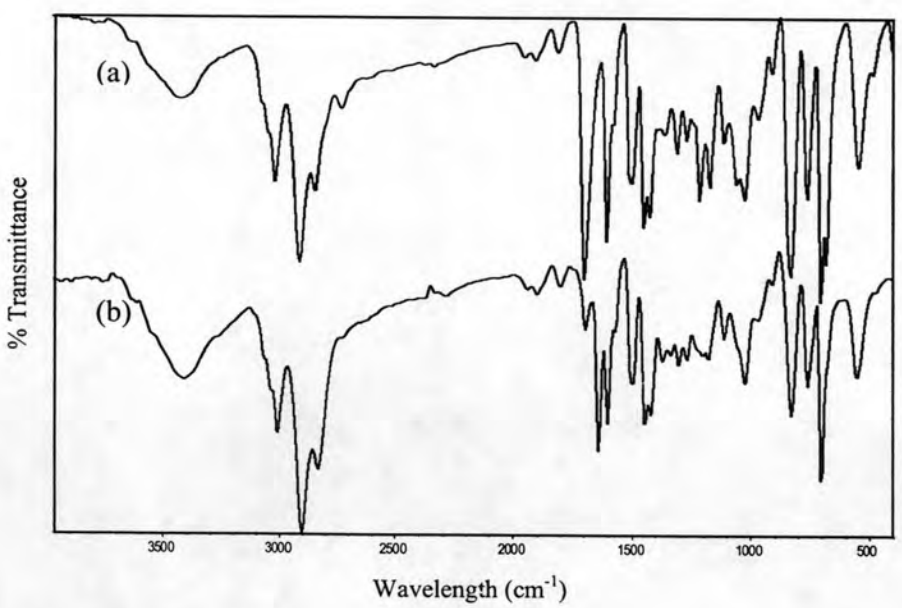

Figure 4.7 FT-IR spectra of the reaction mixture of CHO-PS-DVB with AEEE at reaction time (a) 0 hr and (b) 6 hrs.

At appropriate reaction time, the amounts of AEEE were studied with the same series as the amount of AEEE. The FT-IR spectra of the products were shown in Figure 4.8. The intensity of the C=O absorption band slightly decreased when the amount of AEEE increased. Thus, the amount of AEEE at 2.65 mmol/g was an enough amount since there was significant decreasing in intensity of C=O absorption band.

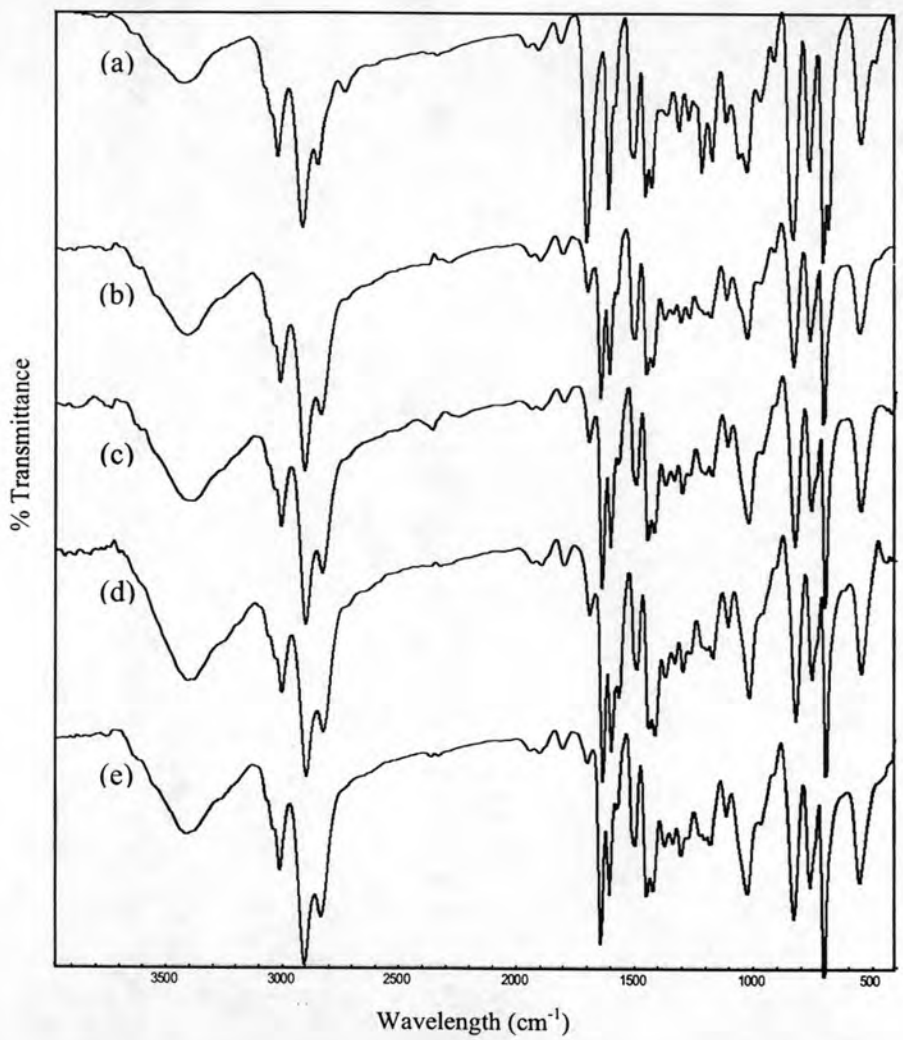

Figure 4.8 FT-IR spectra of the reaction mixture of CHO-PS-DVB with AEEE at different amount of AEEE (a) 0 (b) 2.65 (c) 3.32 (d) 3.87, and (e) 4.42 mmol/g resin.

To study of the effect of reaction temperature towards the completeness of the reaction, the experiment was done at the same way as the study the effect of reaction temperature in preparation AEPE-PS-DVB. The experimental results were shown in

Figure 4.9. The intensity of C=O absorption band of each amount of AEPE slightly decreased, comparing with the results in Figure 4.8. In addition, there was not significant decreasing in intensity of C=O absorption band when the amount of ligand increased. However, the reaction was preferably refluxed for more completion.

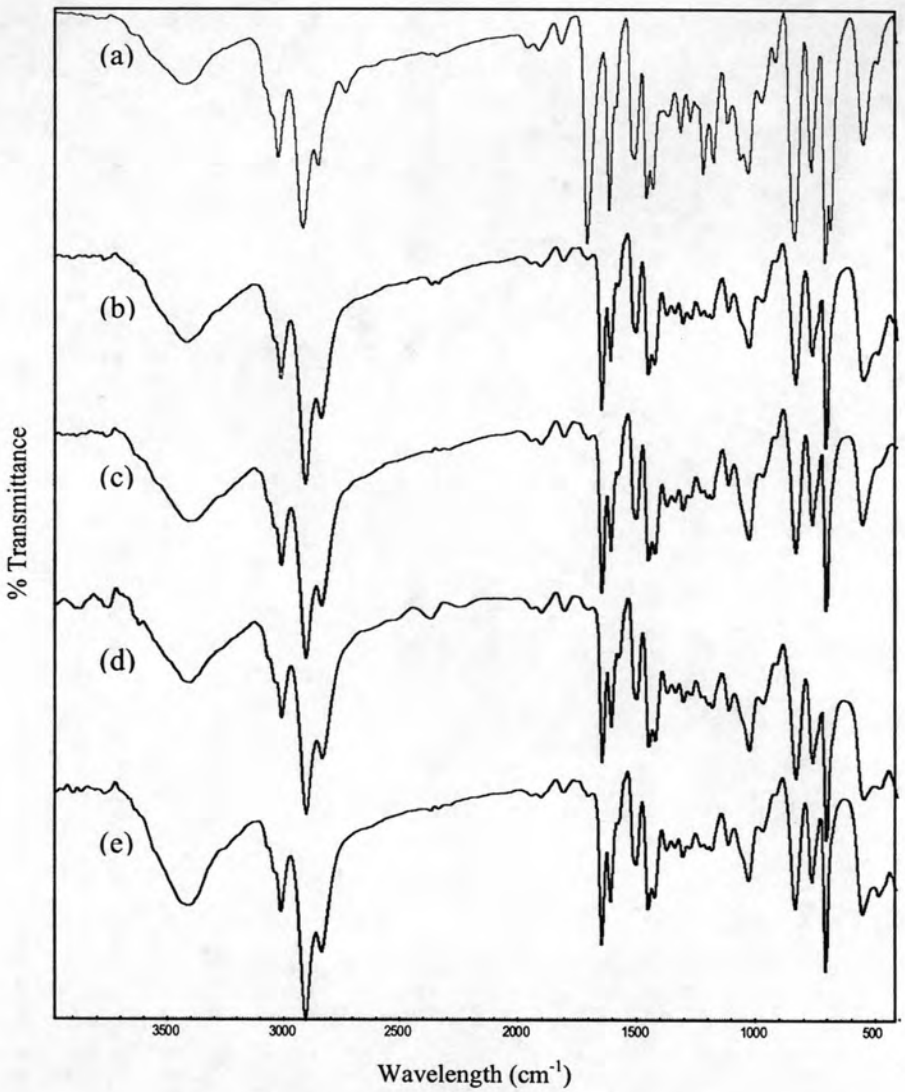

Figure 4.9 FT-IR spectra of the reaction mixture of CHO-PS-DVB with AEEE at 50 °C (a) 0 (b) 2.65 (c) 3.32 (d) 3.87, and (e) 4.42 mmol/g resin.

4.3.3 Polystyrene containing Schiff base TETA ligand, TETA-PS-DVB

TETA was used as received without purifying and its FT-IR, ^{1}H-NMR and ^{13}C-NMR were showed in Figure A.7-A.9. TETA-PS-DVB was synthesized from the reaction between TETA and CHO-PS-DVB as shown in Scheme 4.7.

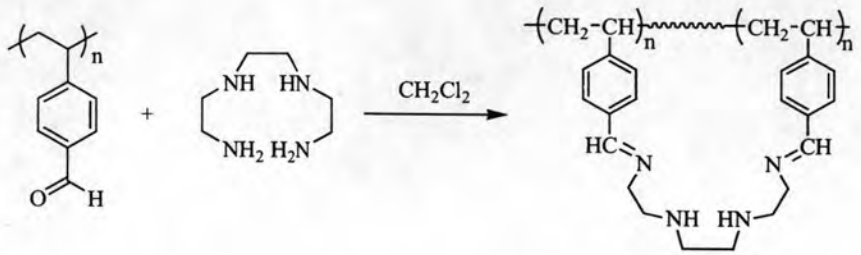

Scheme 4.7 Preparation of TETA-PS-DVB.

The reaction time used of 6 hours in the preparation of TETA-PS-DVB was applied, chosen from the preparation of AEPE-PS-DVB. So, the conditions studied in the preparation of TETA-PS-DVB were only the amount of TETA and the temperature of the reaction. FT-IR spectra of the products from the reaction of CHO-PS-DVB with TETA at room temperature and the amount of TETA at 2.65 mmol/g was shown in Figure 4.10. The spectrum in Figure 4.10 (b) of the chosen reaction time did not show C=O absorption band. Thus, this reaction time was sufficient for the preparation of TETA-PS-DVB.

However, in the study of the amount of TETA (Figure 4.11) and the temperature of the reaction (Figure 4.12). The FT-IR spectra of the products were not different from previous results in Figure 4.10 (b). So there was no use in increasing the amount of TETA and increasing the temperature of reaction. In conclusion, the preparation of TETA-PS-DVB can be achieved with the amount of TETA at 2.65 mmol/g, the reaction time at 6 hours and at room temperature.

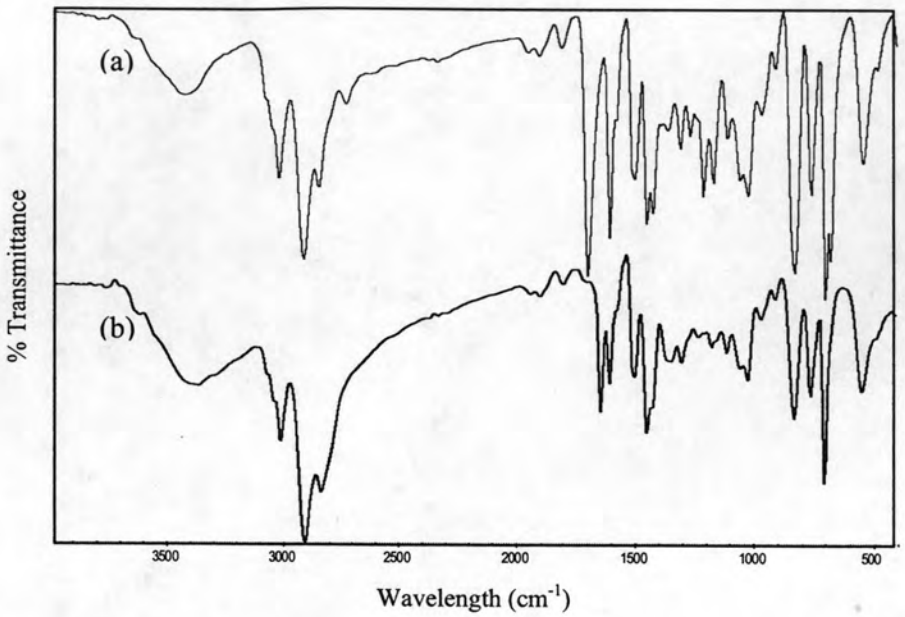

Figure 4.10 FT-IR spectra of the reaction mixture of CHO-PS-DVB with TETA at reaction time (a) 0 hr and (b) 6 hrs.

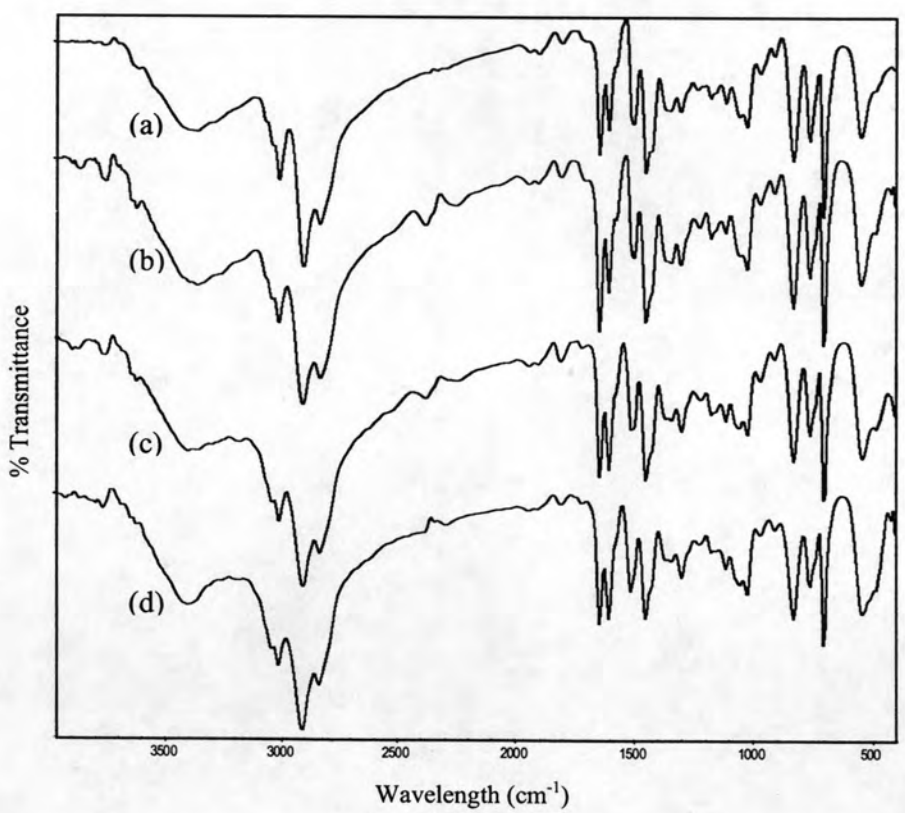

Figure 4.11 FT-IR spectra of the reaction mixture of CHO-PS-DVB with TETA at different amount of TETA (a) 0 (b) 2.65 (c) 3.32 (d) 3.87, and (e) 4.42 mmol/g resin.

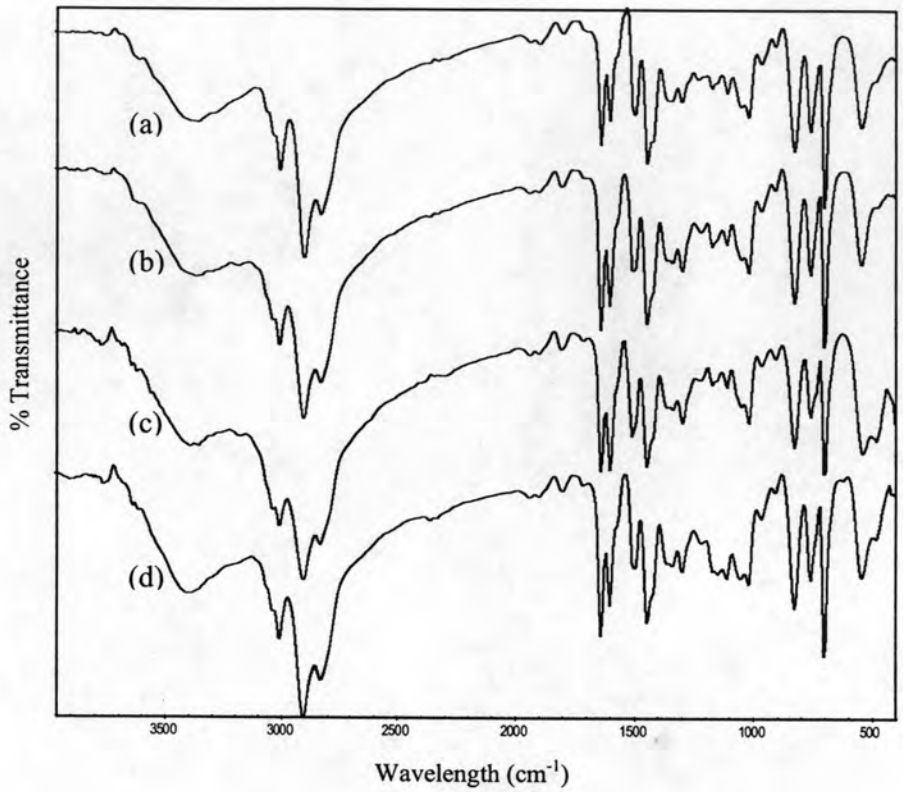

Figure 4.12 FT-IR spectra of the reaction mixture of CHO-PS-DVB with TETA at 50 °C (a) 0 (b) 2.85 (c) 3.32 (d) 3.87, and (e) 4.42 mmol/g resin.

4.4 Characterization of chelating polymers

The final chelating polymers were also characterized by elemental analysis, FT-IR, FT-Raman spectroscopy and thermogravimetric analysis.

4.4.1 Elemental analysis

The elemental analysis results of all three chelating resin were shown in Table 4.2. Nitrogen content of AEPE-PS-DVB and AEEE-PS-DVB was similar. TETA-PS-DVB has more nitrogen content than both other resins, which agrees with the structure of its ligand. The estimated amount of ligand in resulting resins was calculated on the basis on nitrogen content. By this method, the estimated amount of ligand in AEPE-PS-DVB, AEEE-PS-DVB and TETA-PS-DVB was 0.657, 0.486 and 0.798 mmol/g, respectively.

Table 4.2 Elemental analysis results of AEPE-PS-DVB, AEEE-PS-DVB and TETA-PS-DVB

Sample	C (%)	H (%)	N (%)	N/C
CHO-PS-DVB	80.91	7.85	-	-
AEPE-PS-DVB	77.32	7.22	1.84	0.0238
AEEE-PS-DVB	77.65	7.61	1.36	0.0175
TETA-PS-DVB	79.16	8.54	4.47	0.0565

4.4.2 FT-IR

FT-IR spectra of all final chelating resins were shown in Figure 4.13.

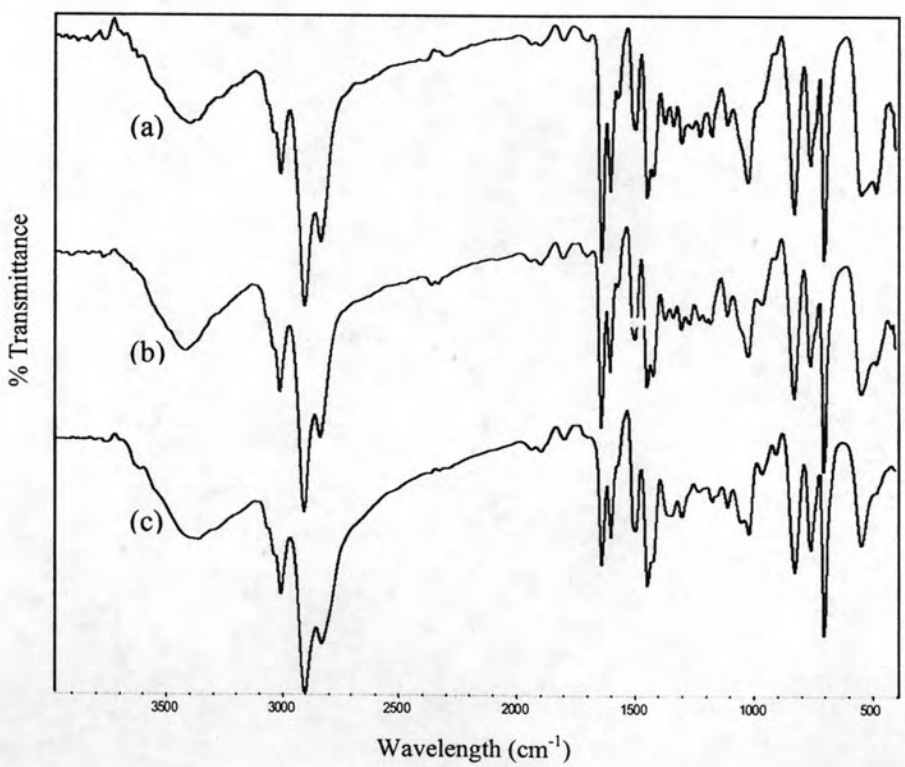

Figure 4.13 FT-IR spectra of (a) AEPE-PS-DVB (b) AEEE-PS-DVB and (c) TETA-PS-DVB.

4.4.3 FT-Raman

Raman spectra of three chelating resins showed similar results as FI-TR spectra. Raman spectra of chelating resins were shown in Figure 4.14. The spectra of all chelating resins were almost similar with the spectrum of CHO-PS-DVB but there was the appearance of important peaks such as: C=N vibration at 1642 cm^{-1} and the disappearance of C=O stretching peak at 1698 cm^{-1}. However, there was remained some Cl group by observing the weak intensity of C-Cl peak at 636, 673 cm^{-1}.

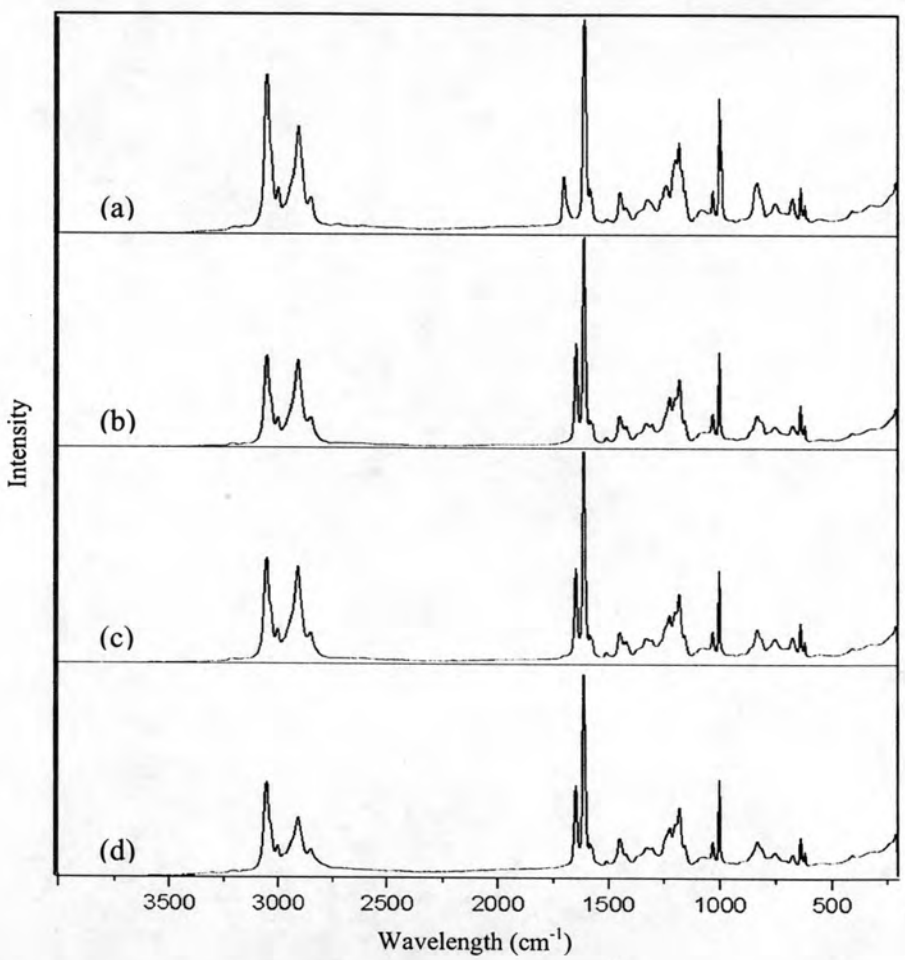

Figure 4.14 Raman spectra of (a) CHO-PS-DVB (b) AEPE-PS-DVB (c) AEEE-PS-DVB and (d) TETA-PS-DVB.

4.4.4 TGA

TGA curves of final chelating resins were displayed in Figure 4.15. TGA curves of chelating resins were the same pattern as CHO-PS-DVB but they showed lower weight loss than the starting resin. All chelating resins showed maximum weight loss around 400-500 °C which might be a degradation of polymeric backbone (Figure 4.15 (b)). From Figure 4.15 (a), it was observed that CHO-PS-DVB thermogram showed approximately 8% weight loss in the region of 150-250 °C. While for AEPE-PS-DVB and AEEE-PS-DVB thermograms showed the weight loss at 240-310 °C, but the percentage weight loss of the former was 1% more than the latter one. This observation corresponds to the structure of the ligands that AEPE has more molecule weight than the AEEE one. For TETA-PS-DVB, the weight loss in this region could not be observed. TGA thermograms indicate that chelating resins were more thermally stable than CHO-PS-DVB. The order of stability can be listed as TETA-PS-DVB > AEEE-PS-DVB > AEPE-PS-DVB > CHO-PS-DVB.

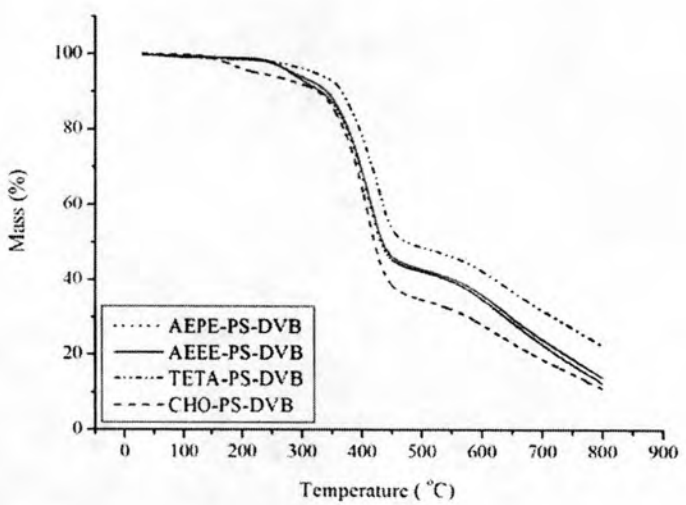

(a)

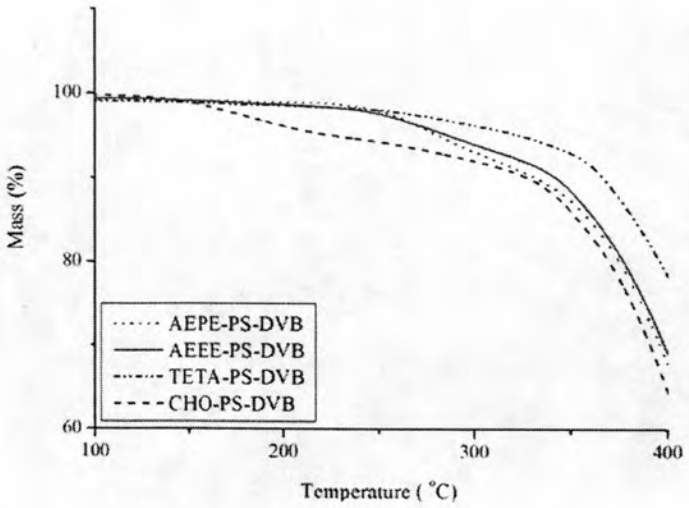

(b)

Figure 4.15 TGA thermograms of CHO-PS-DVB, AEPE-PS-DVB, AEEE-PS-DVB and TETA-PS-DVB: (a) total thermograms and (b) 100-400 °C.

4.4.5 Ninhydrin test

Ninhydrin method was used to detect terminal primary amine (uncoupled terminal amine group of the chelating ligands). The color of CHO-PS-DVB beads and the ninhydrin solution remained their color (yellow solution), this result agreed with the structure of CHO-PS-DVB which had not free amine group. However, in testing of all chelating resins, the color of their beads and the solution turned into brownish yellow solution. The expected color change indicated that there were some remaining free terminal amine groups of the chelating ligands in the PS-DVB beads. The experimental results of ninhydrin test are shown in Table 4.3.

Table 4.3 Ninhydrin test results

Sample	Color of bead	Color of solution
Ninhydrin	-	yellow
CHO-PS-DVB	pale yellow	yellow
AEPE-PS-DVB	brownish yellow	brownish yellow
AEEE-PS-DVB	brownish yellow	brownish yellow
TETA-PS-DVB	brownish yellow	brownish yellow

4.5 Metal adsorption study

Metal adsorption property of the chelating resins was studied in batch method. The studied metals were Pb(II), Cu(II), Cd(II), Zn(II), Ni(II), Co(II) and Cr(III). The initial concentrations of each metal were different and described in each result later. The adsorption of metal ions with chelating ligand moiety onto the resins is based on chelation, the pH of solution is one of the factors in chelation because most chelating ligands are conjugated bases of weak acid groups and they have a very strong affinity for hydrogen ions. Thus, the parameters influencing the adsorption efficiency was investigated only pH of solution. The pH of solution was varied ranging from 1-7, the pH above 7 was not performed due to precipitation of metal hydroxide. In addition, in many research works, the extraction time was done between 15-60 minutes. So in this experiment, the extraction time was selected at 1 hour to ensure the equilibrium between metal ions and chelating ligand moiety in polymer.

The possible chelate structure between metal ions and chelating resins were proposed that metal ions would bind to the nitrogen and sulfur atom of the chelating ligand moiety on the resins to form tetradentate metal complex as shown in Figure 4.16.

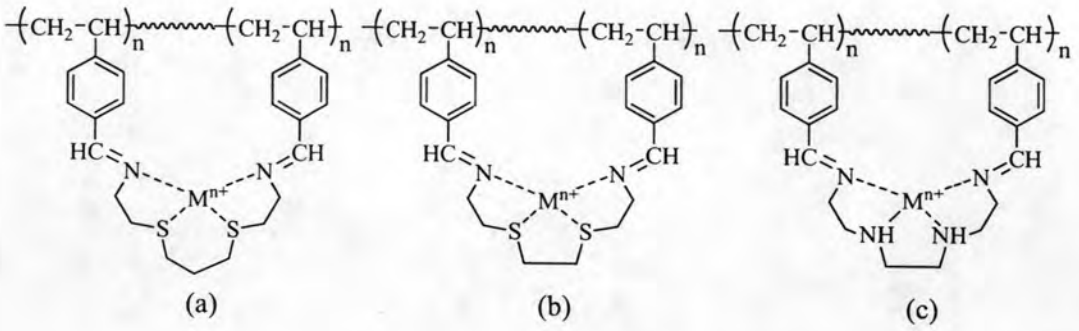

(a) (b) (c)

Figure 4.16 Proposed chelate structures of metal ions with (a) AEPE-PS-DVB, (b) AEEE-PS-DVB and (c) TETA-PS-DVB.

The metal sorption (mg/g resin) of the metal retained on the sorbents was calculated from the difference between the starting amounts of each metal (mg) and the amount of metal (mg) left in the filtrate according to Equation 4.1.

$$\text{Metal sorption} = \frac{N_s - N_f}{m} \quad \text{.....(4.1)}$$

where N_s = the starting amount of each metal (mg)

N_f = the amount of metal left in the filtrate (mg)

m = mass of sorbent (g)

4.5.1 Pb(II)

The results of Pb(II) adsorption were illustrated in Figure 4.17. The initial concentration of Pb(II) was 5 ppm. From the experimental results, the Pb(II) sorption of all chelating resins increased when the pH of solutions increased. In acidic solution, donor atoms (nitrogen and sulfur atom) in chelating moiety that act as an electron donor might be protonated, resulting in positive charge of donor atoms and their ability to bind with Pb(II) ion was very low. When pH of solution was lifted, the protonated donor atoms might be deprotonated and thier ability to bind with Pb(II) ion was revived, resulting in higher metal sorption capacity. However, at pH 3 and pH 4, TETA-PS-DVB sorbed Pb(II) more than the two others chelating resins. Pb(II) that was the biggest metal ion in this research was sorbed by TETA-PS-DVB better. In

addition, Pb(II) ion is a borderline lewis acid that prefers to bind with nitrogen atom rather than sulfur atom. At pH higher than 4, this phenomenon was not affected. By observing the trends of metal sorption of AEPE-PS-DVB and AEEE-PS-DVB, the sorption behaviors of both resins were similar. The optimum pH values on Pb(II) sorption of AEPE-PS-DVB, AEEE-PS-DVB and TETA-PS-DVB were 5-7, 5-7 and 4-6, respectively. Metal sorption capacity at optimum pH of AEPE-PS-DVB, AEEE-PS-DVB was slightly higher than TETA-PS-DVB.

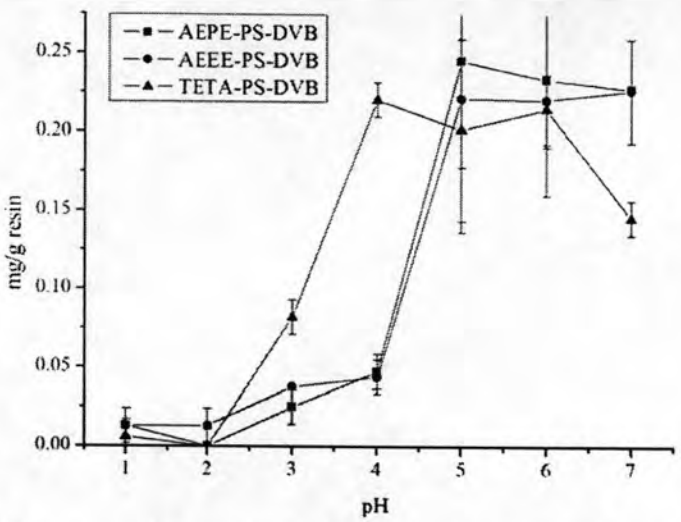

Figure 4.17 Effect of solution pH on Pb(II) sorption onto chelating resins (n=3).

4.5.2 Cu(II)

The results of Cu(II) adsorption were illustrated in Figure 4.18. The initial concentration of Cu(II) was 3 ppm. The sorption of Cu(II) of all chelating resins, except TETA-PS-DVB, increased when the pH of solutions increased. The effect of pH to the sorption of chelating resins can be discussed in the same way as Pb(II) sorption. The trends of metal sorption of AEPE-PS-DVB and AEEE-PS-DVB were similar. However, metal sorption at pH 3 of AEEE-PS-DVB and TETA-PS-DVB was slightly higher than nearby pH 2 and 4 which not quite agreed with discussion. The optimum pH values on Cu(II) sorption of AEPE-PS-DVB, AEEE-PS-DVB and TETA-PS-DVB were 5-7, 5-7 and 7, respectively. Due to the nature of N donor atoms in TETA-PS-DVB, the ligand moiety in this resin can be classified between

borderline and hard ligand. Cu(II), a borderline/soft cation, therefore was not the preferable ion to be chelated by such ligand.

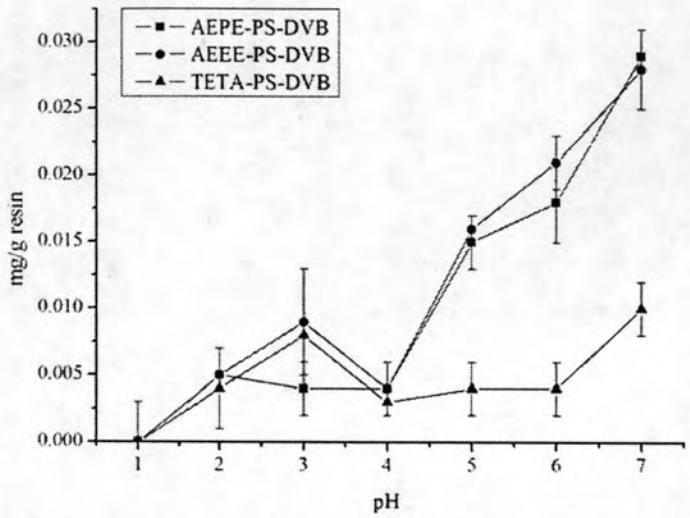

Figure 4.18 Effect of solution pH on Cu(II) sorption onto chelating resins (n=3).

4.5.3 Cd(II)

The results of Cd(II) adsorption were illustrated in Figure 4.19. The initial concentration of Cd(II) was 1 ppm. The sorption behaviors of three resins were all the same as Cu(II) sorption. Considering the results, TETA-PS-DVB was sorped Cd(II) in very low amount, probably due to the characteristic of harder (N) donor atoms in chelating ligand moiety of TETA-PS-DVB than sulfur atoms. The optimum pH values on Cd(II) sorption of AEPE-PS-DVB and AEEE-PS-DVB were the same at 6-7.

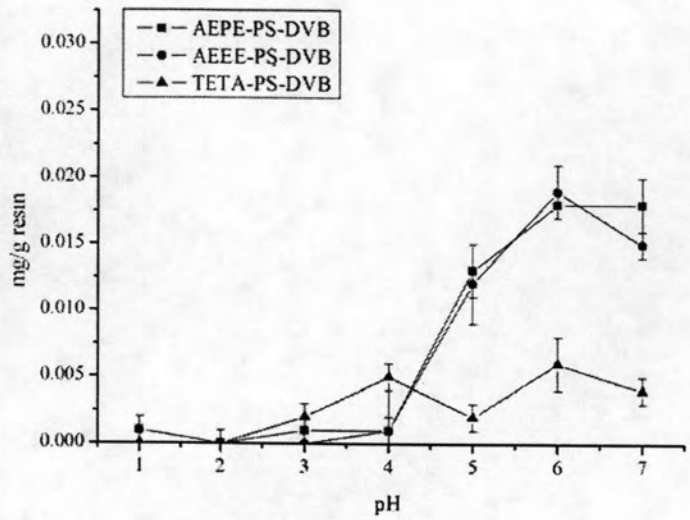

Figure 4.19 Effect of solution pH on Cd(II) sorption onto chelating resins (n=3).

4.5.4 Zn(II)

The results of Zn(II) adsorption were illustrated in Figure 4.20. The initial concentration of Zn(II) was 1.5 ppm. The sorption behaviors of three resins were all the same to Cu(II) and Cd(II) sorption. TETA-PS-DVB sorped Zn(II) in very low amount. The optimum pH values on Zn(II) sorption of AEPE-PS-DVB and AEEE-PS-DVB were the same at 5-6.

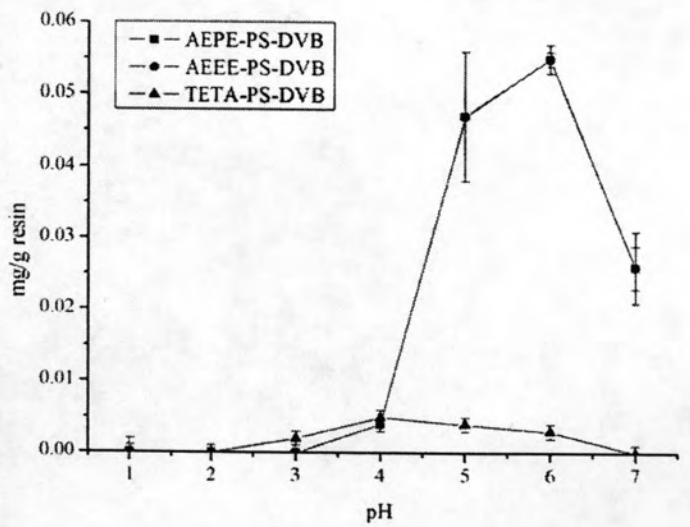

Figure 4.20 Effect of solution pH on Zn(II) sorption onto chelating resins (n=3).

4.5.5 Ni(II)

The results of Ni(II) adsorption were illustrated in Figure 4.21. The initial concentration of Ni(II) was 2 ppm. Ni(II) is borderline cation and possessed affinity for hard (oxygen) and soft ligand (sulfur). However, the experimental data were shown that Ni(II) was sorped by all chelating resins in very low amount. The pH of solution did not affect the sorption.

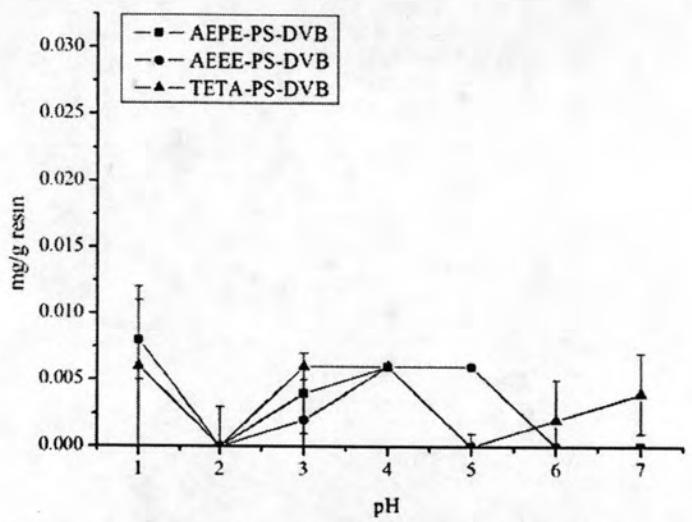

Figure 4.21 Effect of solution pH on Ni(II) sorption onto chelating resins (n=3).

4.5.6 Co(II)

The results of Co(II) adsorption were illustrated in Figure 4.22. The initial concentration of Co(II) was 4 ppm. Co(II) is borderline cation, as same Ni(II), and possessed affinity for hard (oxygen) and soft ligand (sulfur). This was given the same results as Ni(II) sorption. Co(II) was sorped by all chelating resins in very low amount and the pH of solution did not affect its sorption.

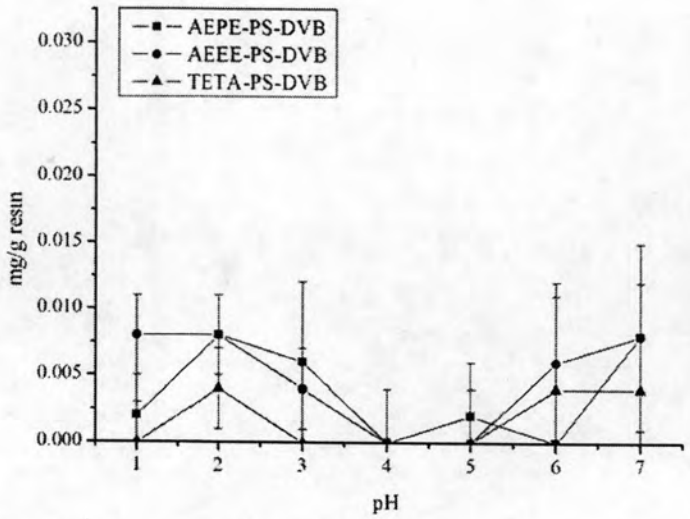

Figure 4.22 Effect of solution pH on Co(II) sorption onto chelating resins (n=3).

4.5.7 Cr(III)

The results of Cr(III) adsorption were illustrated in Figure 4.23. The initial concentration of Cr(III) was 4 ppm. The experimental results were shown that all resins could sorb Cr(III) in very low amount, agreed that Cr(III) is hard cation which cloud not sorb by these borderline and soft donor atoms in chelating ligand moiety. Similarly to Ni(II) and Co(II) sorption behavior, the pH did not affect the sorption of Cr(III).

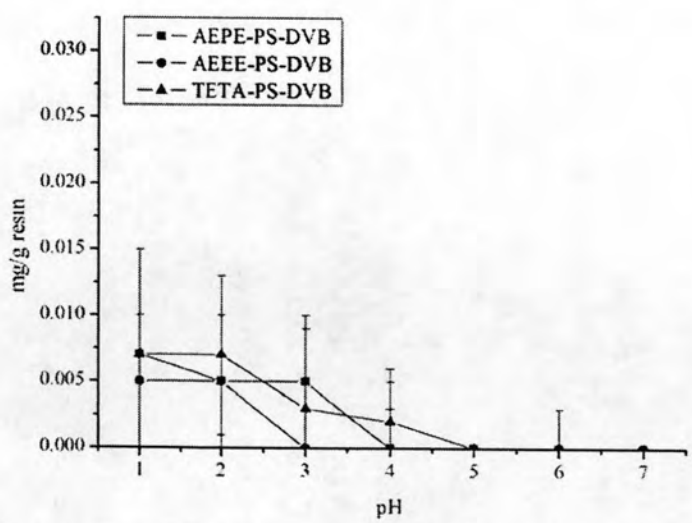

Figure 4.23 Effect of solution pH on Cr(III) sorption onto chelating resins (n=3).

4.5.8 Selectivity of resins

The selectivity can be described approximately in term of ionic or dipole-dipole interactions or complex formation between the metals ions and the ligand moiety on the resins. Although there are other contributions to the complex formation and hence to the equilibrium constant that are:

1) The rearrangement of the donor atoms in chelating ligands.
2) Steric repulsion between the metal ions and the ligands.
3) Competition with the solvent and other ions in solution.

According to the Hard Soft Acid Base Principle (HSAB); hard acids prefer to bind to hard bases and soft acids prefer to bind to soft bases[56], the studied metal ions are classified to Lewis acids. The Lewis acid types and their ionic radius are listed in Table 4.4.

Table 4.4 Classification and ionic radius of the studied metal ions[57]

Ionic radius, r_{ion} (pm)	Hard	Borderline					Soft
	Cr(III)	Co(II)	Ni(II)	Cu(II)	Zn(II)	Pb(II)	Cd(II)
6 coordination	76	79	83	87	88	133	109
4 coordination	-	72	63(sq) 69	71	74	-	92

(sq) means square.

Co(II), Ni(II), Cu(II), Zn(II), and Pb(II) ions were borderline cations that possess affinity for both hard and soft ligands. The order of softness are Pb(II) > Zn(II) > Cu(II) > Ni(II) > Co(II). By considering the types of donor atoms in chelating ligands, they can be classified as soft base ($R_2\underline{S}$) and borderline bases (C=$\underline{N}$, $R_2\underline{N}H$). AEPE-PS-DVB and AEEE-PS-DVB have the same donor atoms (C=N and S) but the cavity size of AEPE-PS-DVB is slightly bigger and more flexible due to the propylene bridge between the two sulfur atoms. In addition, AEEE-PS-DVB and TETA-PS-DVB have nearly the same cavity size of chelating ligand ring but different in donor atoms. The soft Lewis base order could be AEPE-PS-DVB~AEEE-PS-DVB

> TETA-PS-DVB. These characteristics could be assumed to affect the selectivity of the resins towards metal ions. The proper metal ion might be sorbed by the proper chelating resin.

In this experiment, the selectivity of chelating resin can be estimated by observing the maximum metal sorption (in μmol/g of resin) at optimum pH. The results were shown in Figure 4.24-26.

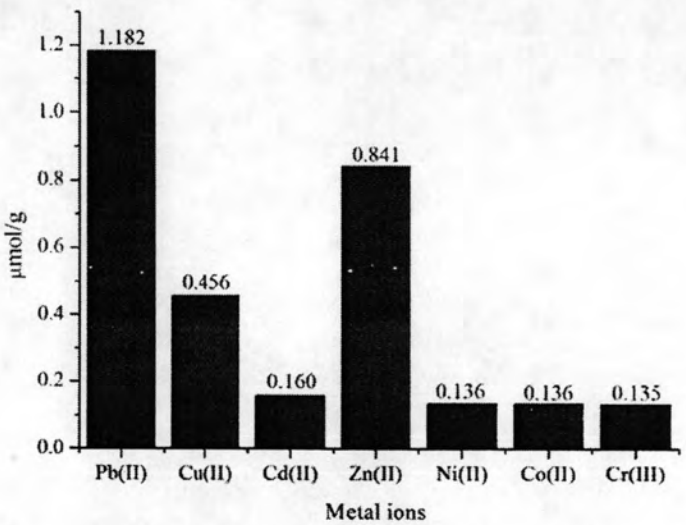

Figure 4.24 Maximum metal sorption of AEPE-PS-DVB.

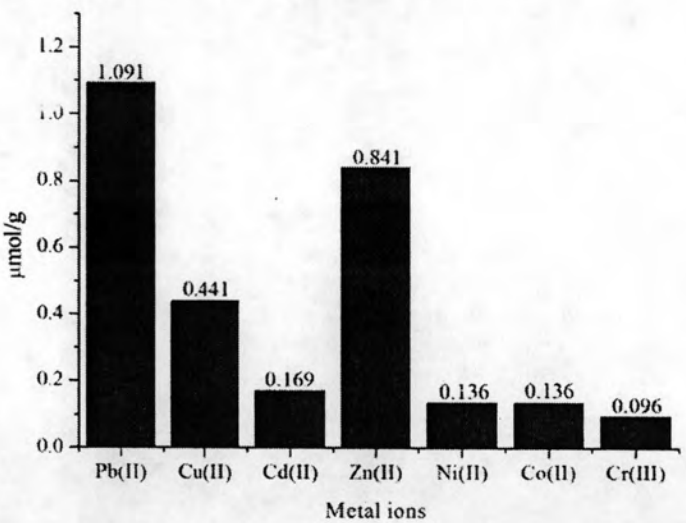

Figure 4.25 Maximum metal sorption of AEEE-PS-DVB.

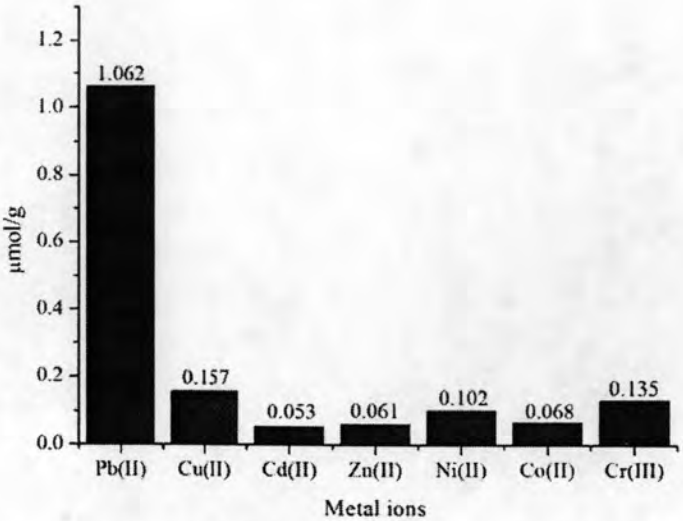

Figure 4.26 Maximum metal sorption of TETA-PS-DVB.

Case of AEPE-PS-DVB and AEEE-PS-DVB

These two resins showed the same sorption behavior. The order of maximum sorption capacity is Pb(II)>Zn(II)>Cu(II)>Cd(II), Co(II), Ni(II), Cr(II). Since Pb(II) ion is the softest-borderline acid, it prefers soft-borderline ligands. While Cr(III) is a hard cation, so it does not prefer to bind with these chelating resins. Zn(II) and Cd(II) ions have a strong affinity for chalcogen ligands, especially RS^- and ArS^- groups, so they generally prefer S. However, Zn(II) ion is borderline acid, while Cd(II) ion is soft acid that does not prefer soft-borderline ligands. Cu(II) ion is a borderline acid and has nearly the same ionic radius to Zn(II) but less soft than Zn(II), thus the selectivity towards Zn(II) is higher the Cu(II) one. For Co(II) and Ni(II) ions, the sorption capacities are very low because the planar geometry of Ni(II) complexes is preferred and the ionic radius of Ni(II) square planar complex (63 pm) is probably too small for complex formation in the ligand cavity, comparing to Zn(II) and Cu(II) whose the ionic radii are 88 and 87 pm, respectively. In case of Co(II), there are more tetrahedral complexes than for other transition metal ions but the ligand geometry is planar. The low sorption of these metal ions might be the ion-exchange mechanism. It can be observed that the order of selectivity is similar to the order of softness of cations.

Case of TETA-PS-DVB

The difference in structure of TETA-PS-DVB and AEEE-PS-DVB is only two nitrogen atoms. TETA-PS-DVB shows the highest selectivity towards Pb(II) ion, while it could rather not adsorb the other ions. This behavior is probable attributed to the appropriate ionic radius of Pb(II) ion that fits the cavity of the ligand.

In this study, it can be remarked that Pb(II) ion is an only one ion which is not transition metal ion. It shows the highest selectivity of all three resins, this might result from the strongest covalent or coordination bonds because of the most electronegative element.